Supporting information for

Exploring Structural Features of Folded Peptide Architectures in the Construction of Nanomaterials

Rajkumar Misra[a], Rahi M. Reja[a], Lagumaddepalli V. Narendra[b], Gijo George[b], Srinivasarao Raghothama[b] and Hosahudya. N Gopi*[a]

[a]Department of Chemistry, Indian Institute of Science Education and Research, Dr-Homi Bhabha Road, Pune-411 008, India; [b]NMR Research, Indian Institute of Science, Bangalore-560 012, India. E-mail: hn.gopi@iiserpune.ac.in

Table of Contents

Peptide Synthesis:

The N-acetylated peptides were synthesized on a MBHA Knorr amide resin at 0.25 mmol scale by manual synthesis method. The peptide couplings were carried out in NMP by standard Fmoc protocol using HBTU/HOBt as coupling reagents. Fmoc deprotection was accomplished by a solution of 20% piperidine in DMF. N-acetylation of peptides was carried out using acetic anhydride/pyridine (1:9). Peptide cleavage from the resin was achieved by treatment of the resin with a mixture of trifluoroacetic acid (TFA)/ triisopropylsilane/water (90:5:5) for 2 h. The resin was filtered with additional TFA (5 mL) and concentrated. The crude peptide was then precipitated by cold diethyl ether (30 mL) and isolated by centrifugation. The precipitate was re-dissolved in 5 mL of 1:1 mixture of MeOH/H_2O and then lyophilized to give a fine white solid. Then crude peptides were purified by reversed-phase HPLC using C18 column (5 μm, 10 X 250 mm). The gradient applied was from 95% A to 95% B in 30 min; where A was water and B was methanol, at a flow rate of 2 mL/min. Pure fractions of peptide were collected by monitoring UV-Vis at 254 nm. Further, peptides were characterized by MALDI-TOF/TOF.

Size distribution analysis of peptide vesicles using DLS:

Mean diameter of the peptide vesicles in aqueous methanol solution was measured by dynamic light scattering (DLS) experiment using 90° scattering angle. Samples were prepared by dissolving 1mg/mL of peptide in 6:4 MeOH / H_2O.

SEM, TEM, AFM study: SEM sample were prepared by depositing peptide solution (4μL, 1mg/mL in 6:4 MeOH / water) on SiO_2/Si substrate, dried at room temperature and imaged it. Before each and every experiment, fresh solutions have been made (for P3 immediately drop casted the solution onto a SiO_2/Si substrate to avoid the aggregation). Similarly **TEM** sample were prepared by deposing peptide solution (4μL, 1mg/mL in 6:4 MeOH/water) on copper grid, dried at room temperature and imaged it. For **AFM**, samples were drop casted on mica, dried at room temperature and imaged.

Effect of physical, chemical and enzyme stability on the structure of vesicles: To test pH sensitivity of the vesicles, we made vesicle solution acidic and basic by adding slowly TFA (to adjust to pH 4) and 5N NaOH (to adjust to pH 9), respectively and imaged it. For thermal stability we drop casted vesicle solution onto a SiO_2/Si substrate and kept it in the oven at

different temperatures and imaged it. The resistance to enzymatic proteolysis of vesicles was investigated by treating them with proteinase K. Proteinase K solution was prepared by dissolving 0.4 mg enzyme in 1 mL 60% methanol/ water and added to the vesicle solution. In order to maintain the proteolytic activity of proteinase K, the solution was incubated for 24 hours at 37 °C. For thermogravimetric analysis (TGA), vesicles solution was lyophilized and TGA was carried out on a Perkin Elmer STA 6000 simultaneous thermal analyzer. The sample was heated in an alumina crucible at a rate of 5 °C min^{-1}.

Carboxyfluorescein encapsulation study: 1.3 mM carboxyfluorescein solution was added to the peptide vesicles solution to make the final concentration 0.1 mM and then kept it over night and dialyzed .

Procedure for fluorescent leakage study: Peptide vesicles (200 μL) loaded with carboxyfluorescein was sealed in dialysis membrane and then 200μL of 5 mM solution of cationic dipeptide in water was added. This dialysis bag was suspended in agitating methanol /water solution. Further, 300μL aliquot of suspension medium was timely collected and quantification of released carboxyfluorescein was carried out.

Fluorescence measurement: Fluorescent measurement experiments were carried out using FluoroMax-4 HORIBA fluorimeter, with 492 nm excitation and 500-650 nm emission range using 2/2 slit and 1 nm data interval. The aliquots (300 μL) obtained from leakage assay were further diluted with 200 μL of methanol.

Laser Scanning Confocal Microscopy Experiments. Carboxyfluorescein entrapped vesicles solution was drop casted on a glass slide, dried and then imaged using OLYMPUS ZX81 laser scanning confocal microscopy.

NMR:

NMR spectra were recorded on 700 MHz spectrometer in CD_3OH solvent. Nearly 3mM peptide concentrations were used. Temperature were maintained at 278 K to move away residual water signal away from C^{α} proton signals and the water suppression power had minimal effect on nearby peptide resonances. Resonance assignments were carried by using TOCSY and ROESY spectra. All 2D spectral widths were 12 ppm with 2048 x 512 time domain points in t2

and t1 domains respectively. Data set was zero filled to 4K x 2K before Fourier transformation. A mixing time of 100ms and 250ms were used for TOCSY and ROESY spectrum respectively. All NMR data were processed offline using TOPSPIN version 2.1 software. Scalar coupling (J) values were directly measured from high resolution 1D recording. Amide proton temperature coefficients (dδ/dT) were measured by recording 1D experiment at definite intervals of 10 degrees (K) in the temperature range of 278-318 K. Concentration dependent NMR spectra were recorded on 500 MHz spectrometer in CD_3OH solvent.

Modeling:

A computer model was generated using discovery studio version 3.5 software based on NMR data. The dihedral angles ϕ and ψ were maintained at near extended values based on $^3J_{NHC^{\alpha}H}$ values and observation of weak d_{NN} and relatively strong $d_{\alpha N}$ NOEs. The θ1 and θ2 dihedrals for the Aic residues were fixed at gauche (*g*) and *trans* (*t*) values so that it agree with the observed NOE pattern. The resultant structure was energy minimized with Powell-Reeves Conjugate Gradient (PRCG) method (Macro Model 10.3) using OPLS2005 force-field. The final structure matched with all NMR parameters.

Table ST 1: Tabulation of chemical shifts along with $^{3}J_{NHC}{}^{\alpha}{}_{H}$ scalar couplings and amide temperature coefficients (dδ/dT) for peptide (**P2**) : Ac-[Phe-Aic]$_3$-Phe-NH_2.

Residue	Chemical shifts (ppm)						$^{3}J_{NHC}{}^{\alpha}{}_{H}$ (Hz)	dδ/dT (ppb)
	NH	$C^{\alpha}H$	$C^{\beta}H$	$C^{\gamma}H$	$C^{\delta}H$	Others		
Acetyl						1.92(CH_3)		
Phe (F1)	8.30	4.45	2.92	-	-	Aromatics 7.24-7.18	7.0	8.3
Aic($^{\gamma}$U2)	7.57	2.04	1.96/1.71	-	1.16/1.02	-	-	7.3
Phe (F3)	8.17	4.46	2.94/2.89	-	-	Aromatics 7.24-7.18	7.4	8.3
Aic($^{\gamma}$U4)	7.56	2.05	1.97/1.72	-	1.17/1.04	-	-	7.3
Phe (F5)	8.19	4.41	2.95/2.88	-	-	Aromatics 7.24-7.18	7.3	8.6
Aic($^{\gamma}$U6)	7.55	2.01	1.86/1.63	-	1.16/1.04	-	-	7.2
Phe (F7)	8.15	4.59	3.12/2.83	-	-	Aromatics 7.24-7.18	8.3	8.1
C-ter. NH_2	7.76/7.19	-	-	-	-	-	-	7.2

Table ST 2: Tabulation of backbone dihedral angles of peptide **P2**, energy minimized model satisfying NMR data.

Residue	**ϕ**	**θ_1**	**θ_2**	**ψ**
Phe_1	-80.92			160.45
Aic_2	179.13	-56.85	-178.27	135.50
Phe_3	-81.37			160.67
Aic_4	179.17	-56.87	-178.33	135.36
Phe_5	-81.35			160.61
Aic_6	179.19	-56.83	-178.21	143.04
Phe_7	-83.51			137.38

Table ST3: Tabulation of chemical shifts along with $^{3}J_{NHC}{}^{\alpha}{}_{H}$ scalar couplings and amide temperature coefficients (dδ/dT) for peptide **P1**.

Residue	Chemical shifts (ppm)						$^{3}J_{NHC}{}^{\alpha}{}_{H}$ (Hz)	dδ/dT (ppb)
	NH	$C^{\alpha}H$	$C^{\beta}H$	$C^{\gamma}H$	$C^{\delta}H$	Others		
Acetyl						1.86(CH_3)		
Aic($^{\gamma}$U1)	7.63	2.18	1.94		1.25 /1.22			6.6
Phe (F2)	8.22	4.46	2.95/2.91	-	-	Aromatics 7.26-7.18	7.0	8.6
Aic($^{\gamma}$U3)	7.59	2.05	1.94/1.72		1.17/1.05	-	-	7.3
Phe (F4)	8.23	4.47	2.96/2.90	-	-	Aromatics 7.26-7.18	7.2	8.8
Aic($^{\gamma}$U5)	7.56	2.04	1.98/1.73		1.16/1.02	-	-	7.0
Phe (F6)	8.20	4.43	2.96/2.88	-	-	Aromatics 7.26-7.18	7.2	8.7
Aic($^{\gamma}$U7)	7.64	2.09	2.04/1.78	-	1.23/1.12	-	-	7.3
C-ter. NH_2	7.61/6.89	-	-	-	-	-	-	6.8

Table ST4: Tabulation of backbone dihedral angles of peptide **P1**, energy minimized model satisfying NMR data.

Residue	**ϕ**	**θ_1**	**θ_2**	**ψ**
Aic_1	179.15	-56.59	-178.12	136.45
Phe_2	-81.37			160.62
Aic_3	179.14	-56.87	-178.33	135.30
Phe_4	-81.35			160.60
Aic_5	179.17	-56.82	-178.20	145.22
Phe_6	-81.60			163.79
Aic_7	-174.01	-55.57	176.48	-143.26

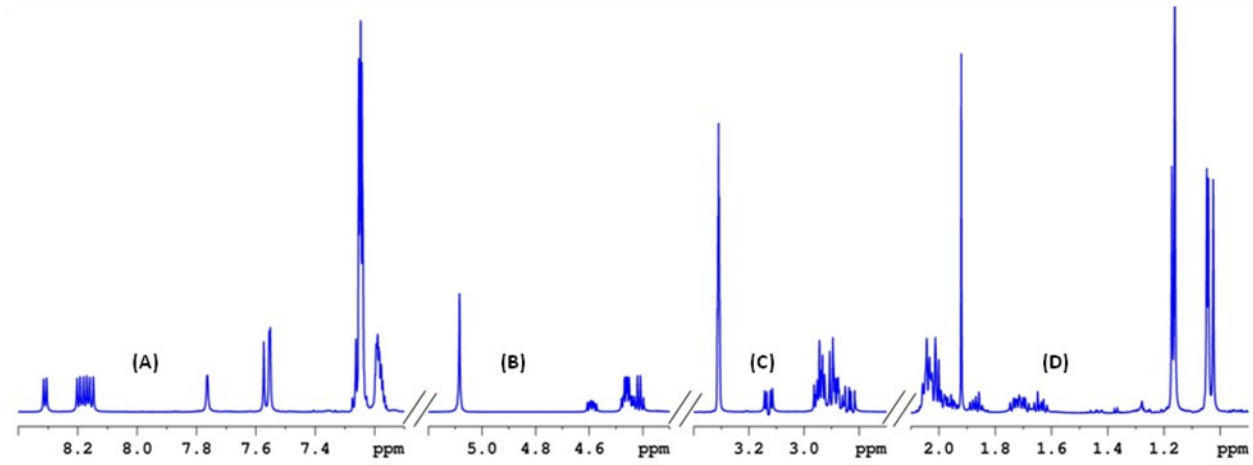

Figure S1: 700 MHz ^{1}H recording of peptide Ac-[Phe-Aic]$_3$-Phe-NH_2(**P2**) in CD_3OH at 278K. The three different regions are (A) Amide and aromatic, (B) residual water and C^{α} protons, (C) C^{β} protons of Phe. (D) Other aliphatic protons including Aib methyls.

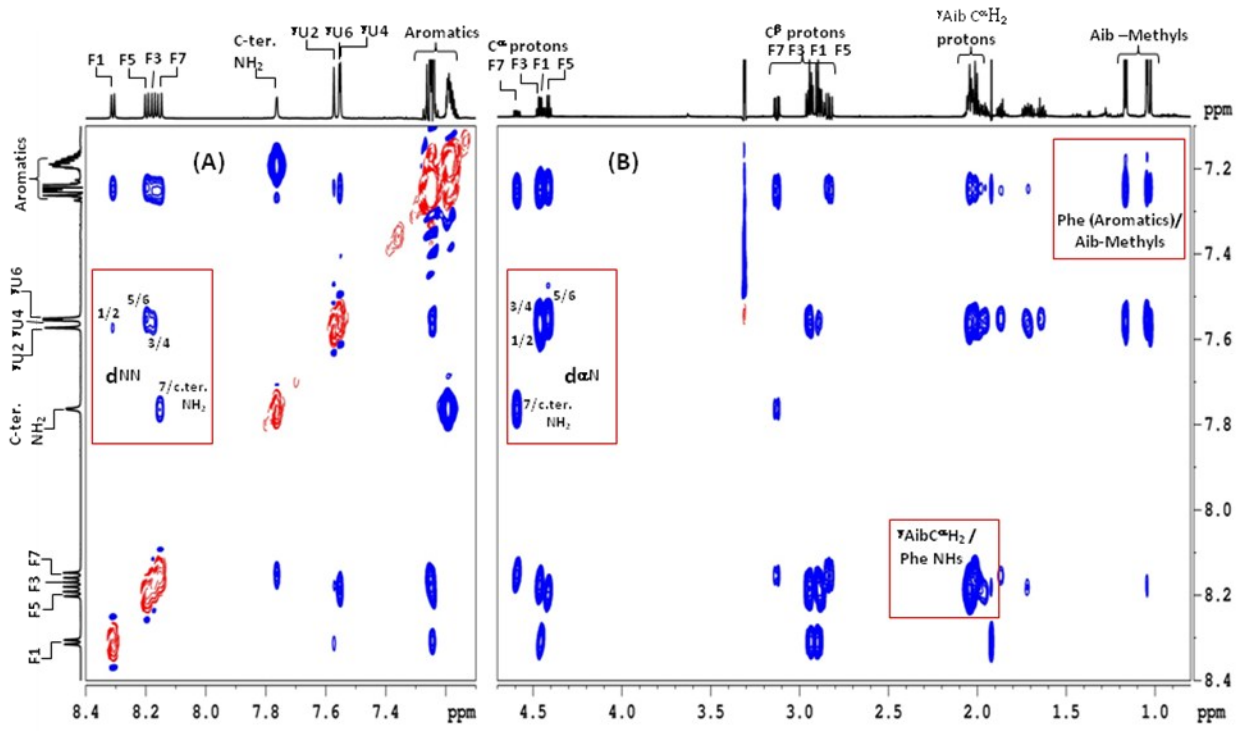

Figure S2: Partial ROESY spectra of **P2**. (A) Amide/aromatic region, (B) Amide/Aromatic-Aliphatic region. d_{NN} and $d_{\alpha N}$ with differential intensities are boxed. So also Aromatics NOEs to Aic methyl's. Most of these NOEs were considered in making a computer energy minimized model of the peptide molecule.

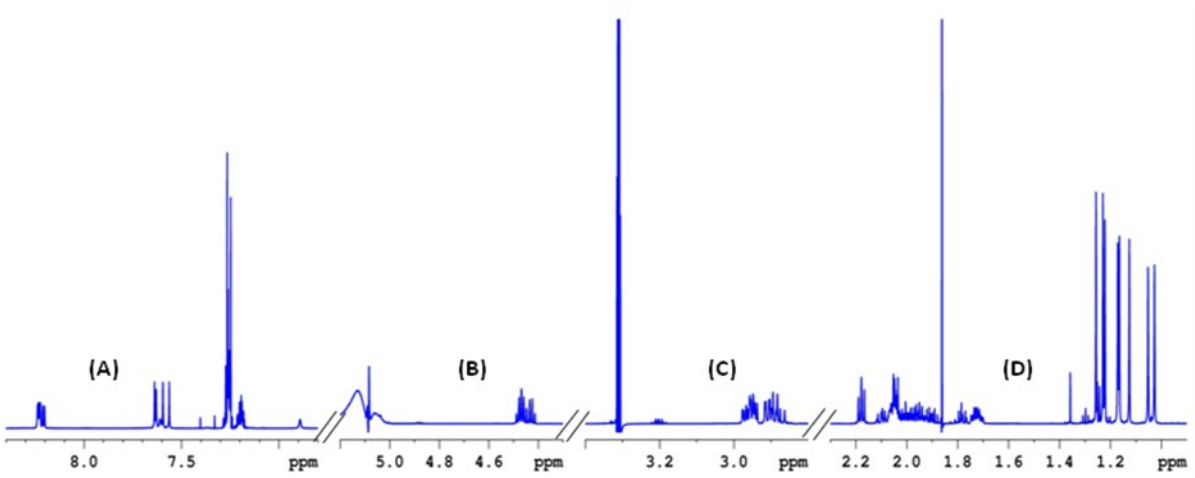

Figure S3: 700 MHz ^{1}H recording of peptide Ac-[Aic-Phe]$_3$-Aic-NH_2 (**P1**)in CD_3OH at 278K. The three different regions are (A) Amide and aromatic, (B) residual water and C^{α} protons, (C) C^{β} protons of Phe. (D) Other aliphatic protons including Aic methyls.

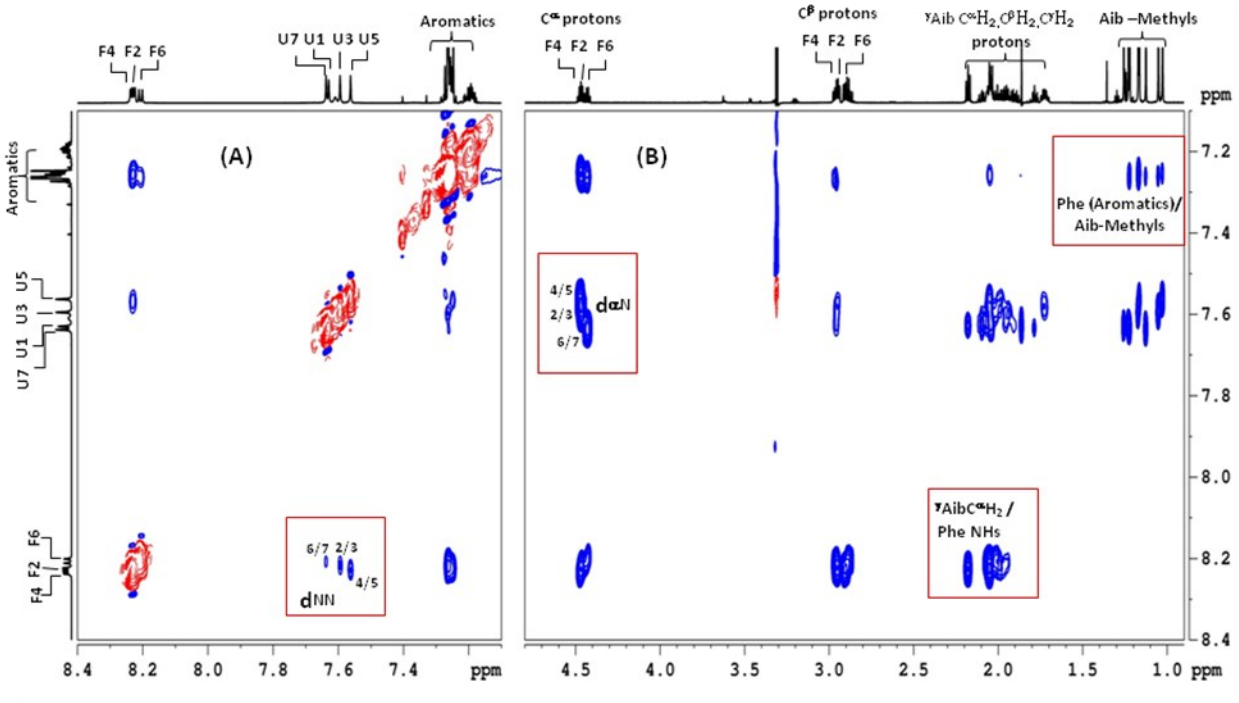

Figure S4: Partial ROESY spectra of **P1**. (A) Amide/aromatic region, (B) Amide/Aromatic-Aliphatic region. d_{NN} and $d_{\alpha N}$ with differential intensities are boxed. So also Aromatics NOEs to Aic methyls. Most of these NOEs were considered in making a computer energy minimized model of the peptide molecule.

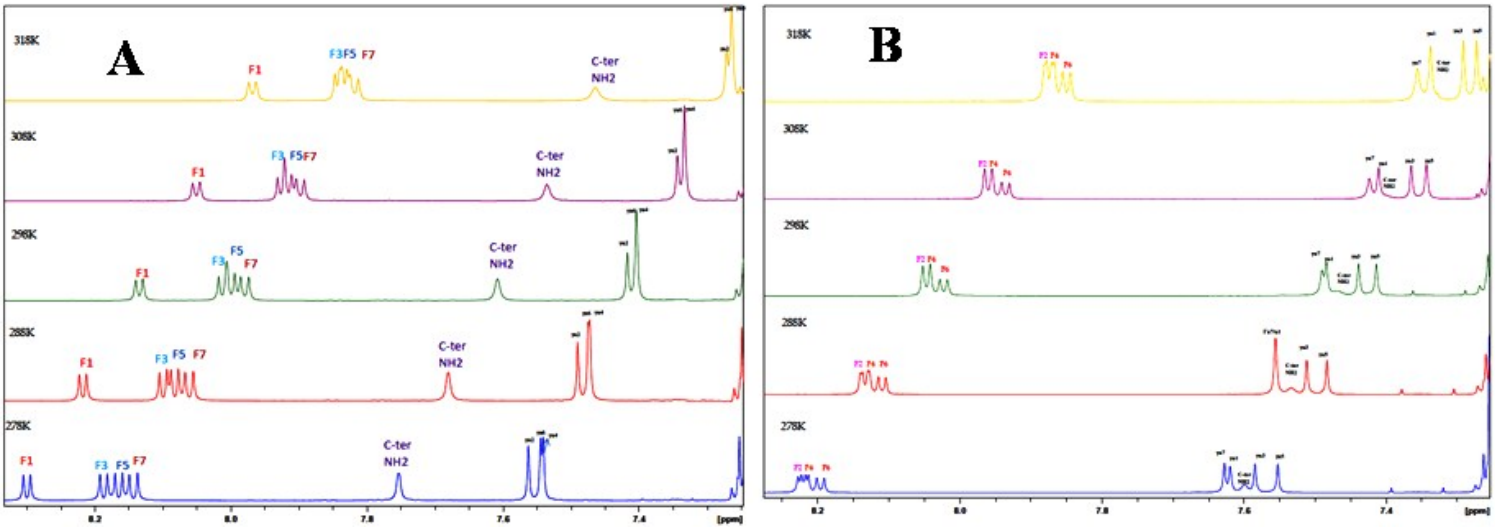

Figure S5. Up field chemical shifts of all amide protons with increasing temperature from 278 K to 308 K. A)Temperature dependent ^{1}H NMR spectra of peptide **P2 .**B) Temperature dependent ^{1}H NMR spectra of peptide **P1.** Spectra were recorded in 700 MHz spectrometer in CD_3OH.

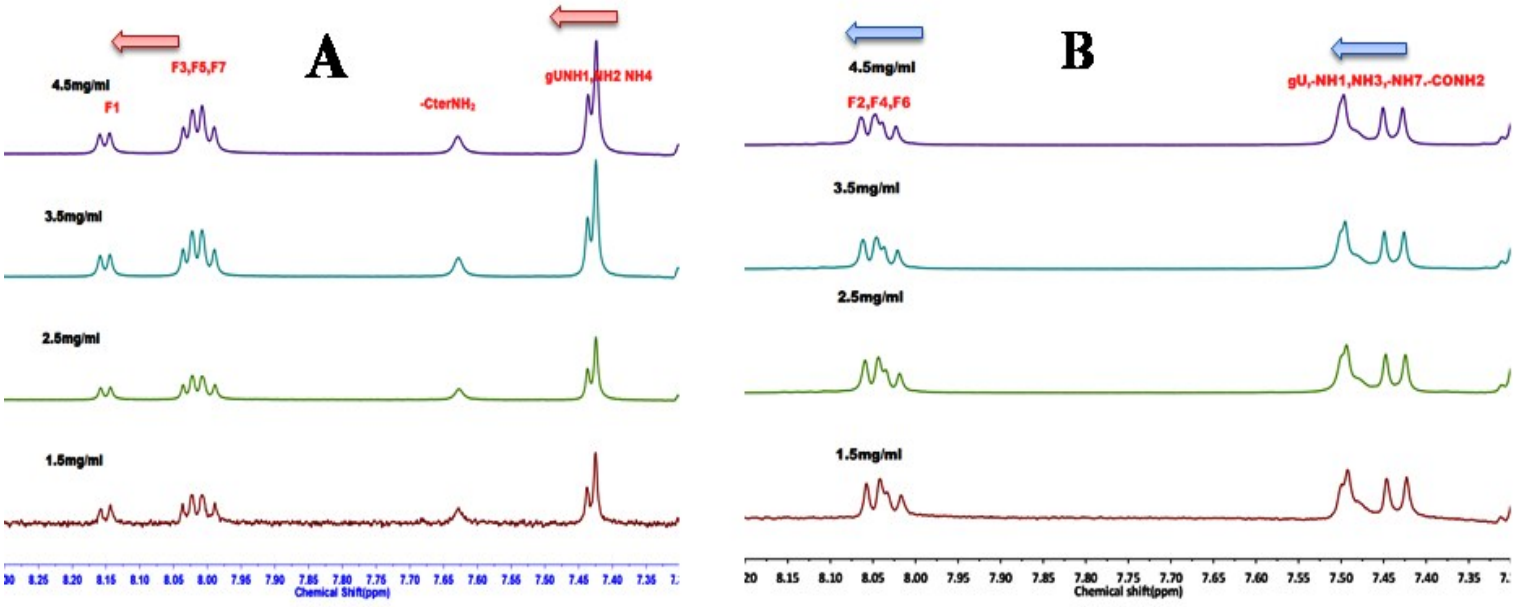

Figure S6. A very slight downfield chemical shift was observed for all the amide protons with increasing the concentration of the peptides. A) Concentration dependent ^{1}H NMR spectra of peptide **P2**. B) Concentration dependent ^{1}H NMR spectra of peptide **P1**. Spectra were recorded on 500 MHz spectrometer in CD_3OH.

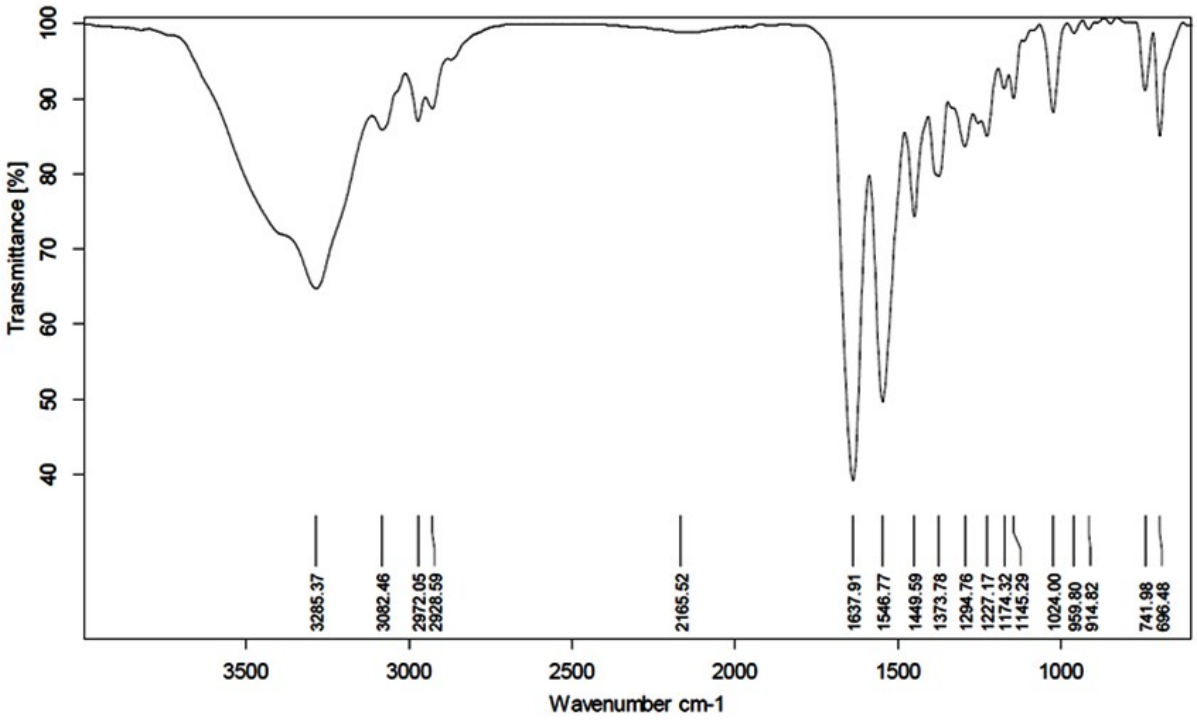

Figure S7. FT-IR spectrum of peptide **P1** recorded using 1mg/mL in methanol water mixture (6:4)

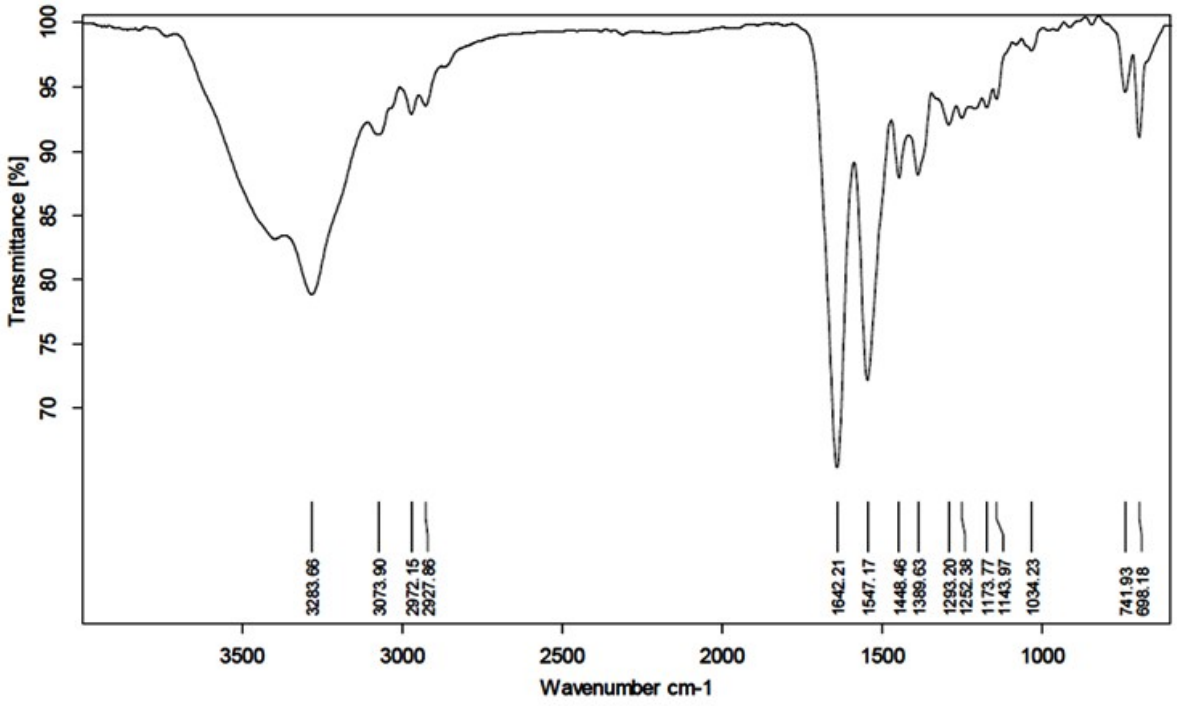

Figure S8. FT-IR spectrum of peptide **P2** recorded using 1 mg/mL in methanol water mixture(6:4)

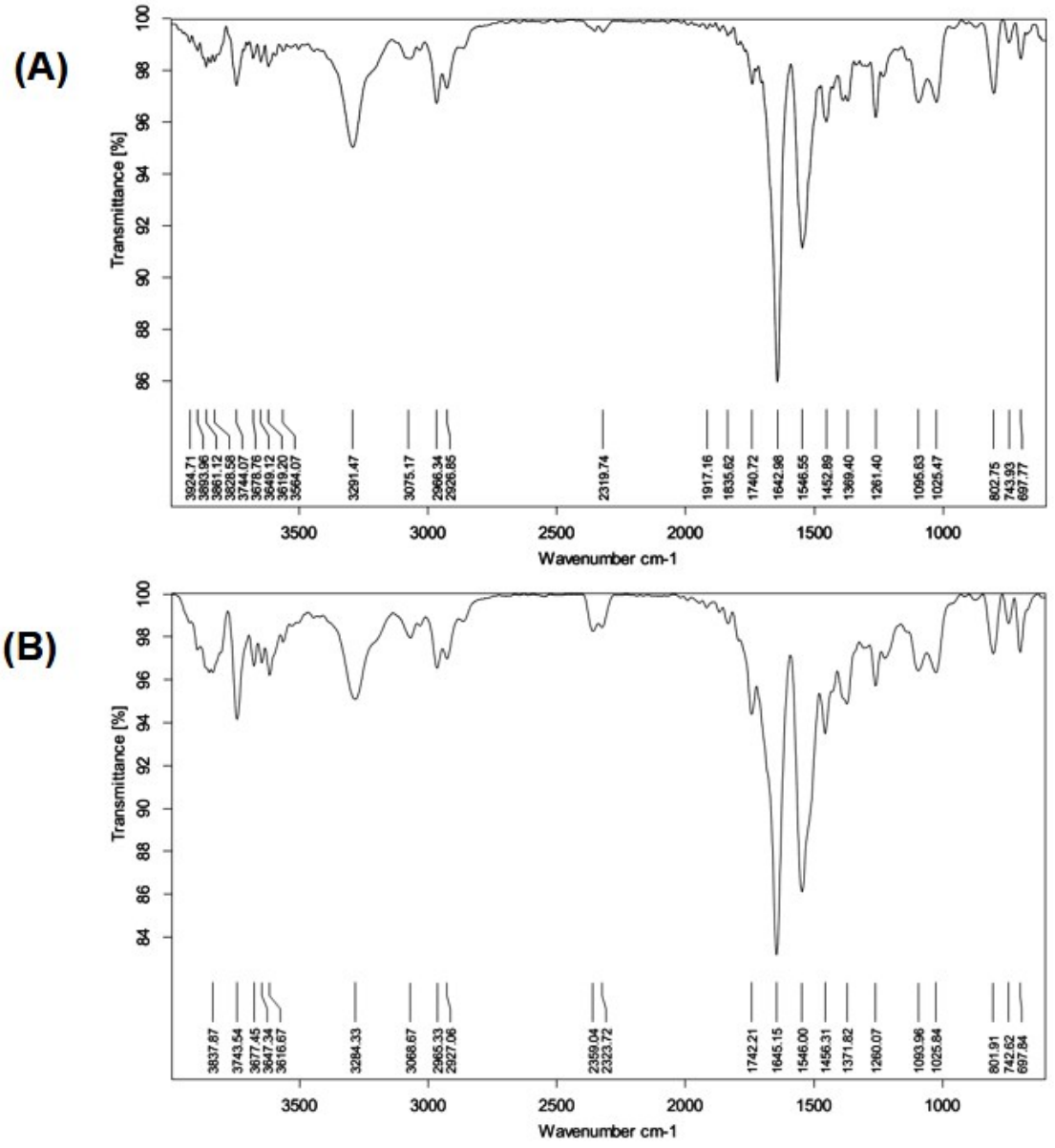

Figure S9: FT-IR spectra of **P1**(A) and **P2**(B) recorded using 0.2 mg/mL in dichloromethane.

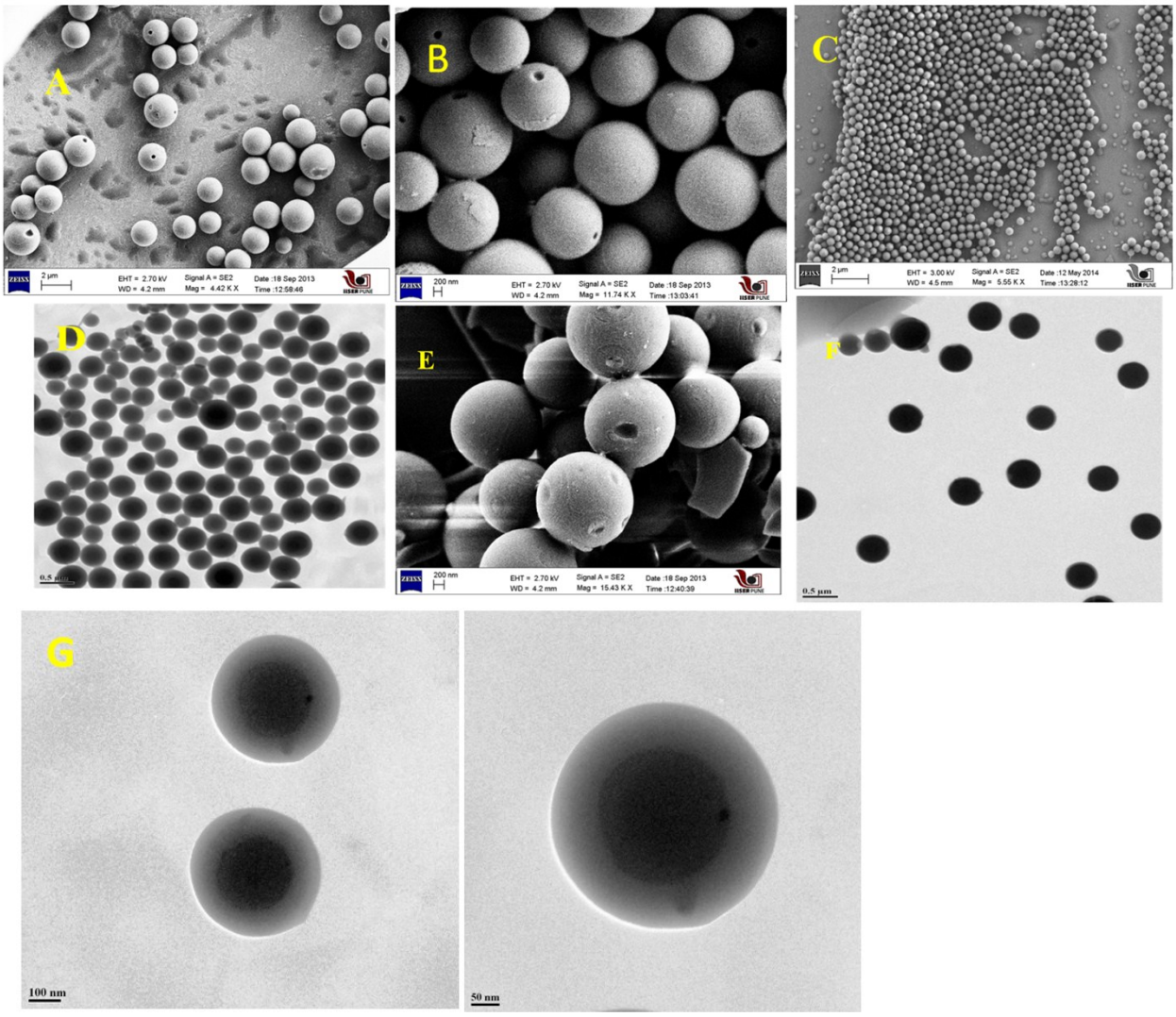

Figure S10. A), B) and C): SEM images of the capsules of peptide **P2** in (6:4) methanol water mixture. D) TEM images of the capsules of peptide **P2.** E) SEM images (E) of the vesicles of peptide **P1** in (6:4) methanol water mixture. F) TEM images of the capsules of peptide **P1. G)**High magnified TEM images of self-assembled capsule from peptide **P2**.

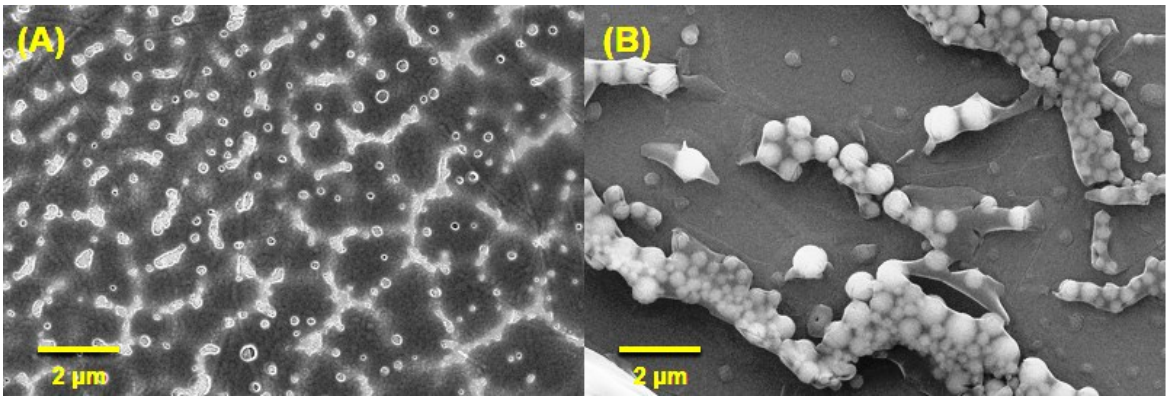

Figure S11. SEM images of **P1** (A) and **P2** (B) in THF water mixture (1:4)

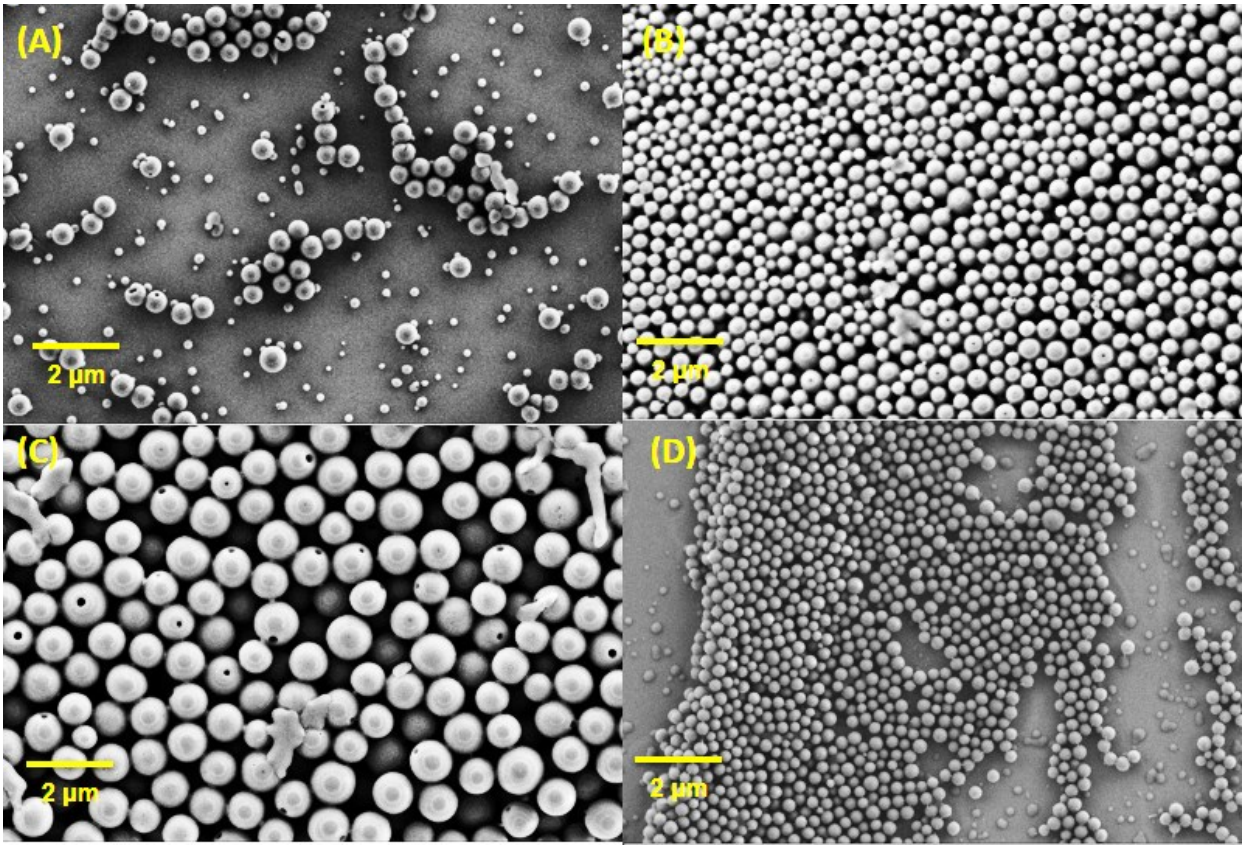

Figure S12. SEM images of **P2** (A) methanol; B) 80% methanol in water; C) 70% methanol in water; D) 60% methanol in water.

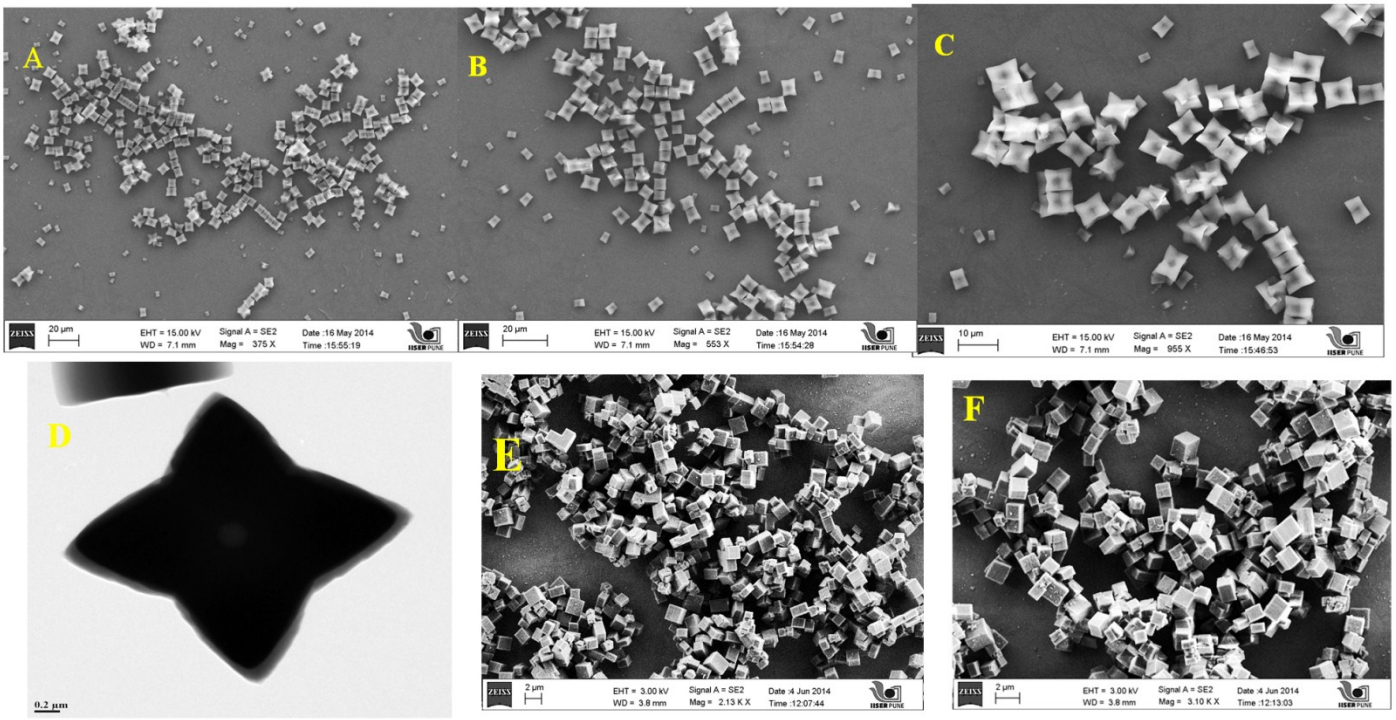

Figure S13. A),B) and C): SEM images of the polyhedrons from peptide **P3** in (6:4) methanol water mixture. D) TEM images of polyhedrons. E) and F): SEM images of polyhedrons of peptide **P3** in (4:6) methanol water mixture.

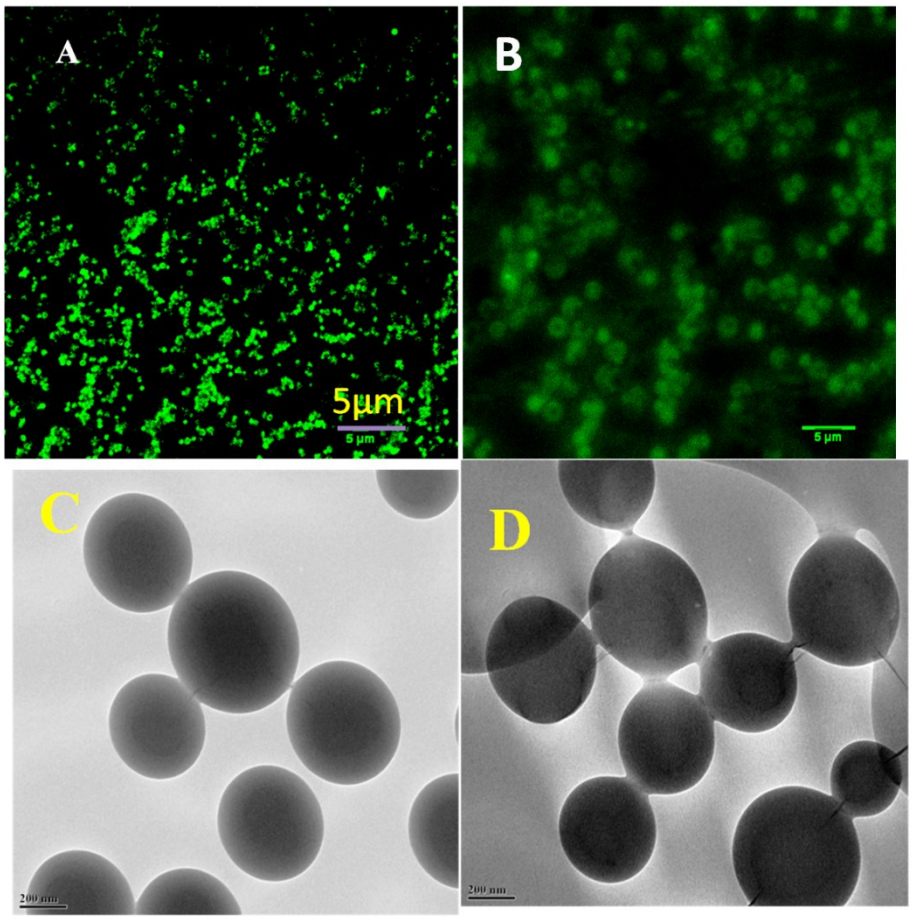

Figure S14: A) and B): The LSCM images of vesicles of peptide **P2** entrapped with carboxyfluorescein (green, λ_{ex} = 517 nm). C) and D): TEM images of vesicles entrapped with carboxyfluorescein.

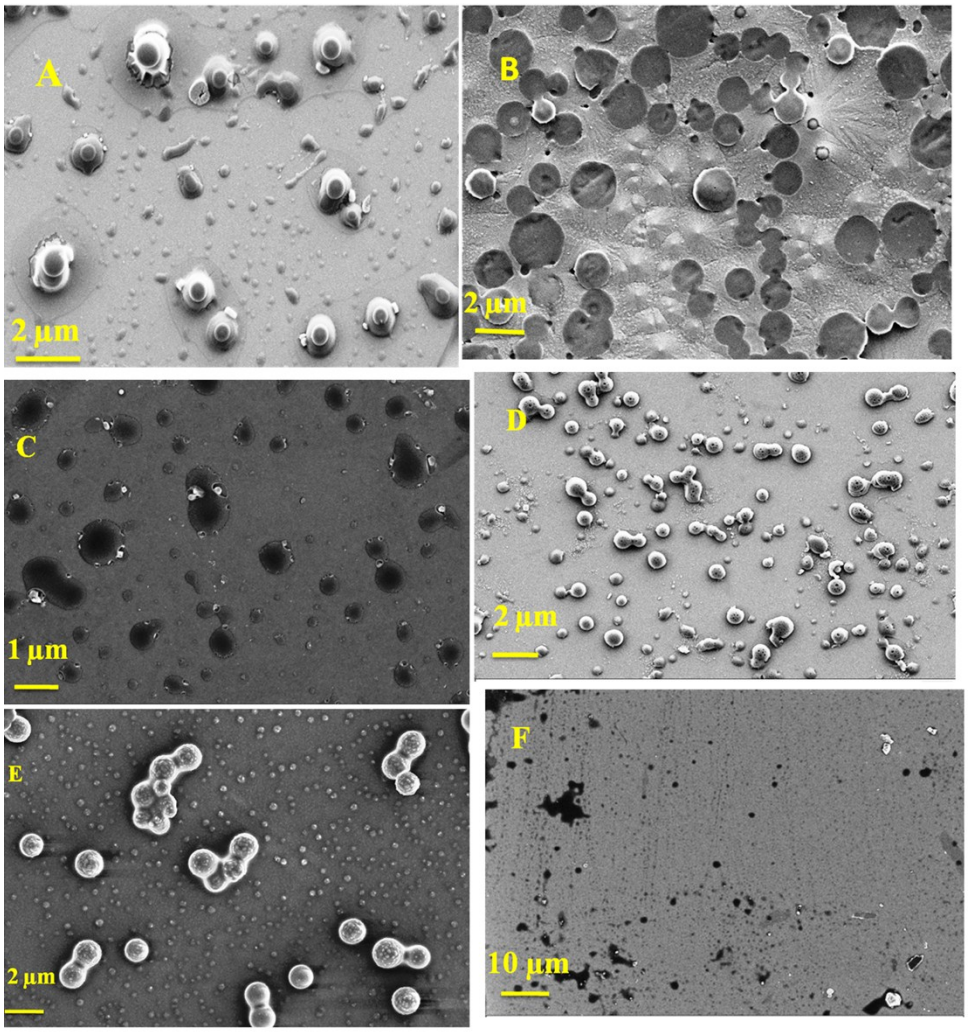

Figure S15. SEM images of peptide vesicles of peptide **P2** with different stimuli. A) At acidic condition; B) Basic condition; C) After heating 100 ^{o}C; D) After heating 150 ^{o}C; E) After treating with Proteinase K; F) After treating with 6 equivalent of Bu_4NBr.

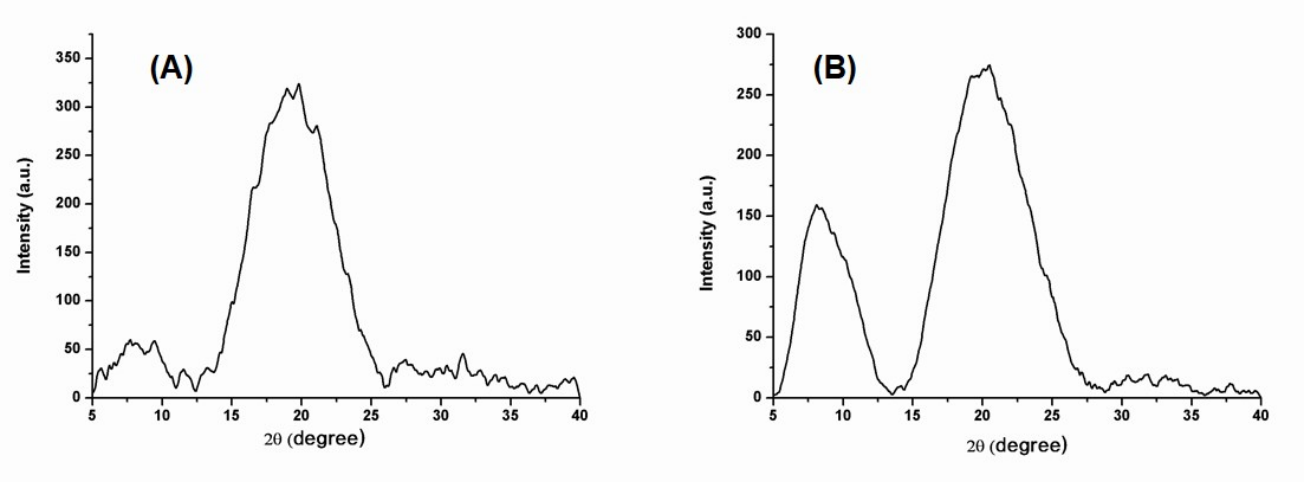

Figure S16: PXRD analysis of peptides **P1** (A) and **P2** (B).

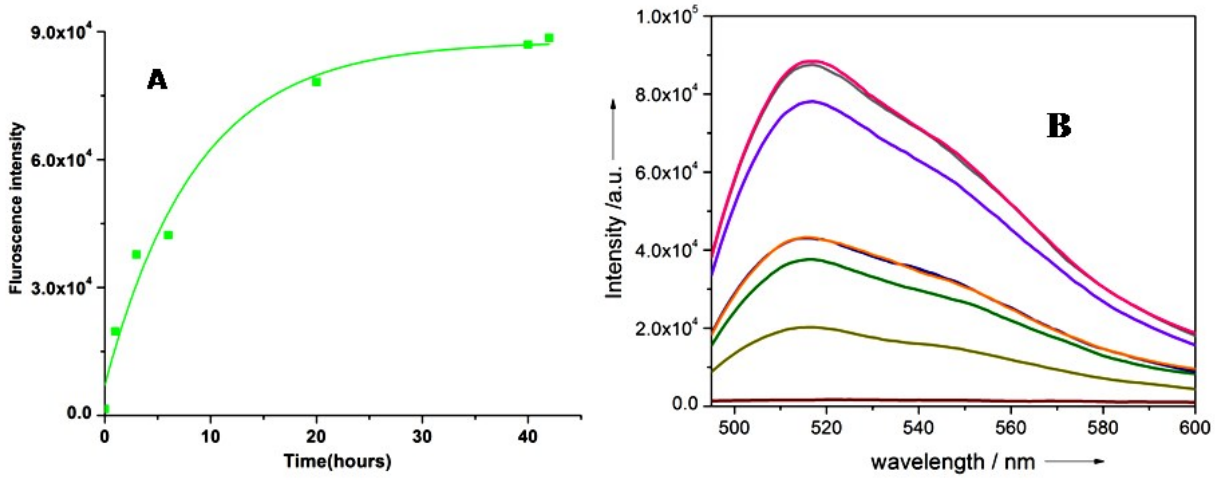

Figure S17. (A) The increasing fluorescence intensity of the solution outside the dialysis tube after the addition of 6 eq. Bu_4NBr into dialysis tube (λ_{ex}= 492nm); (B) Fluorescence emission spectra of carboxyfluorescein (at 517 nm) with increasing intensity after the addition of Bu_4NBr.

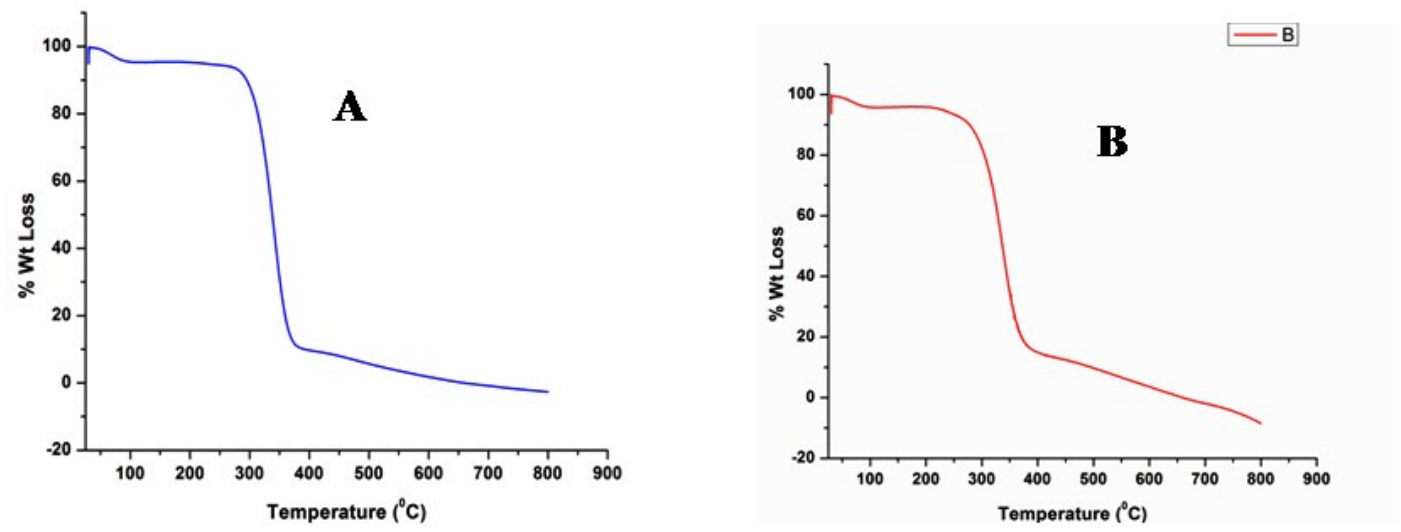

Figure S18. Thermogravimetric thermograms of peptide **P1** and **P2** showing high thermal stability.

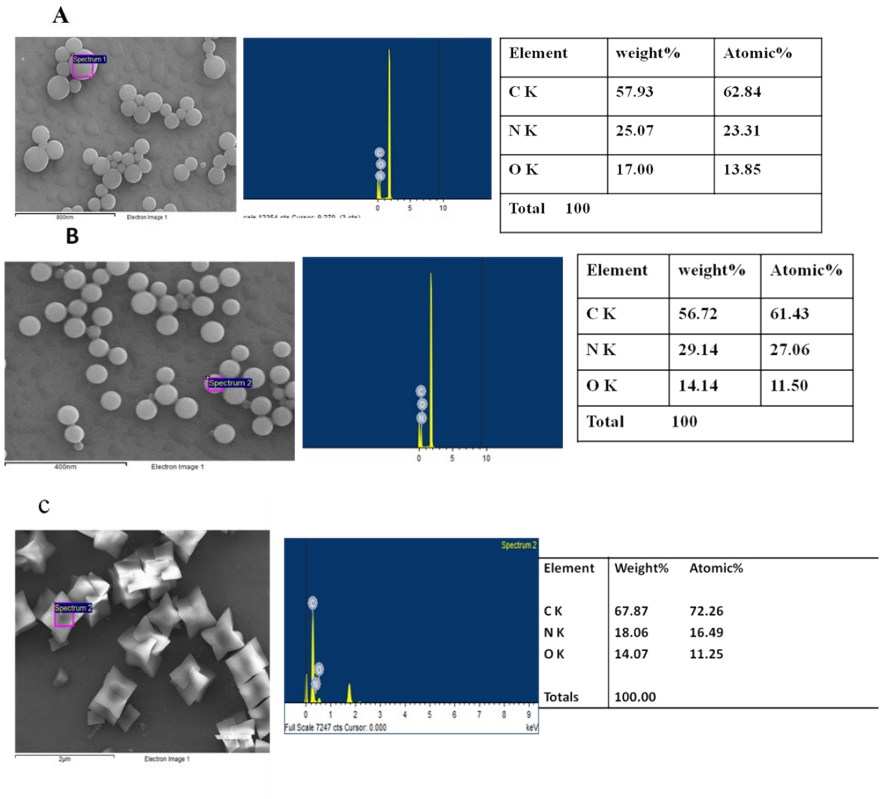

Element	weight%	Atomic%
C K	57.93	62.84
N K	25.07	23.31
O K	17.00	13.85
Total	100	

Element	weight%	Atomic%
C K	56.72	61.43
N K	29.14	27.06
O K	14.14	11.50
Total	100	

Element	Weight%	Atomic%
C K	67.87	72.26
N K	18.06	16.49
O K	14.07	11.25
Totals	100.00	

Figure S19. A) EDAX analysis of peptide **P1;** B) EDAX analysis of peptide **P2;** C) EDAX analysis of peptide **P3**.

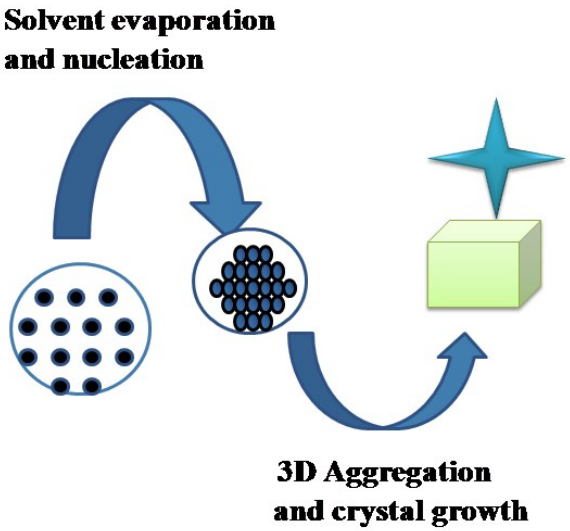

Figure S20. General mechanism of the formation of polyhedrons from the self-assembly of peptide **P3**.

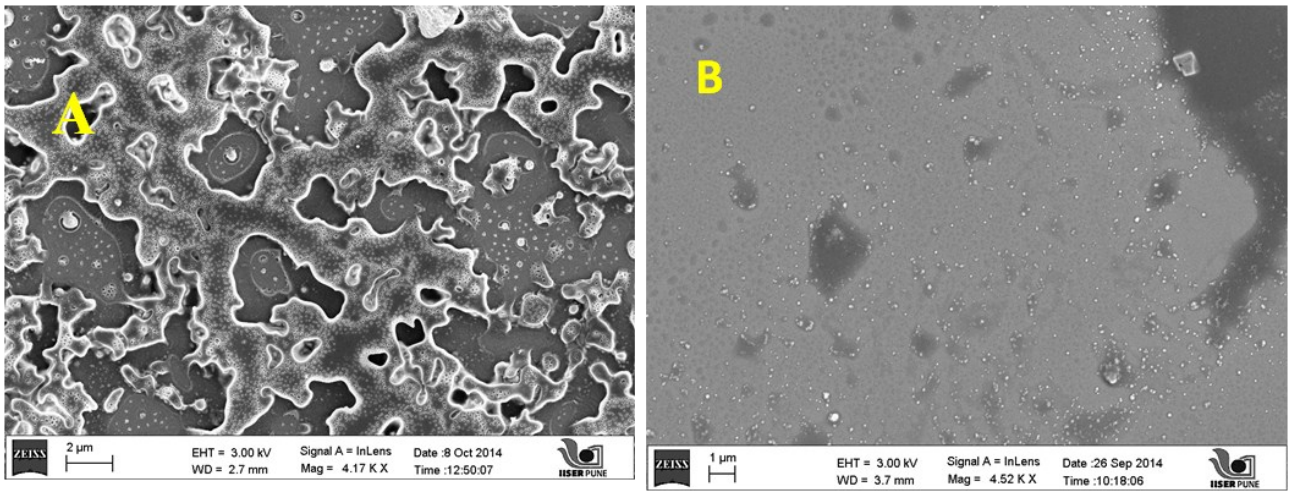

Figure S21. A) and B): SEM imges of peptide after addition of cationic di peptide, Cbz-Lys-Lys-OMe, to the carboxyfluorescein entrapped vesicles.

Mass spectra of peptides

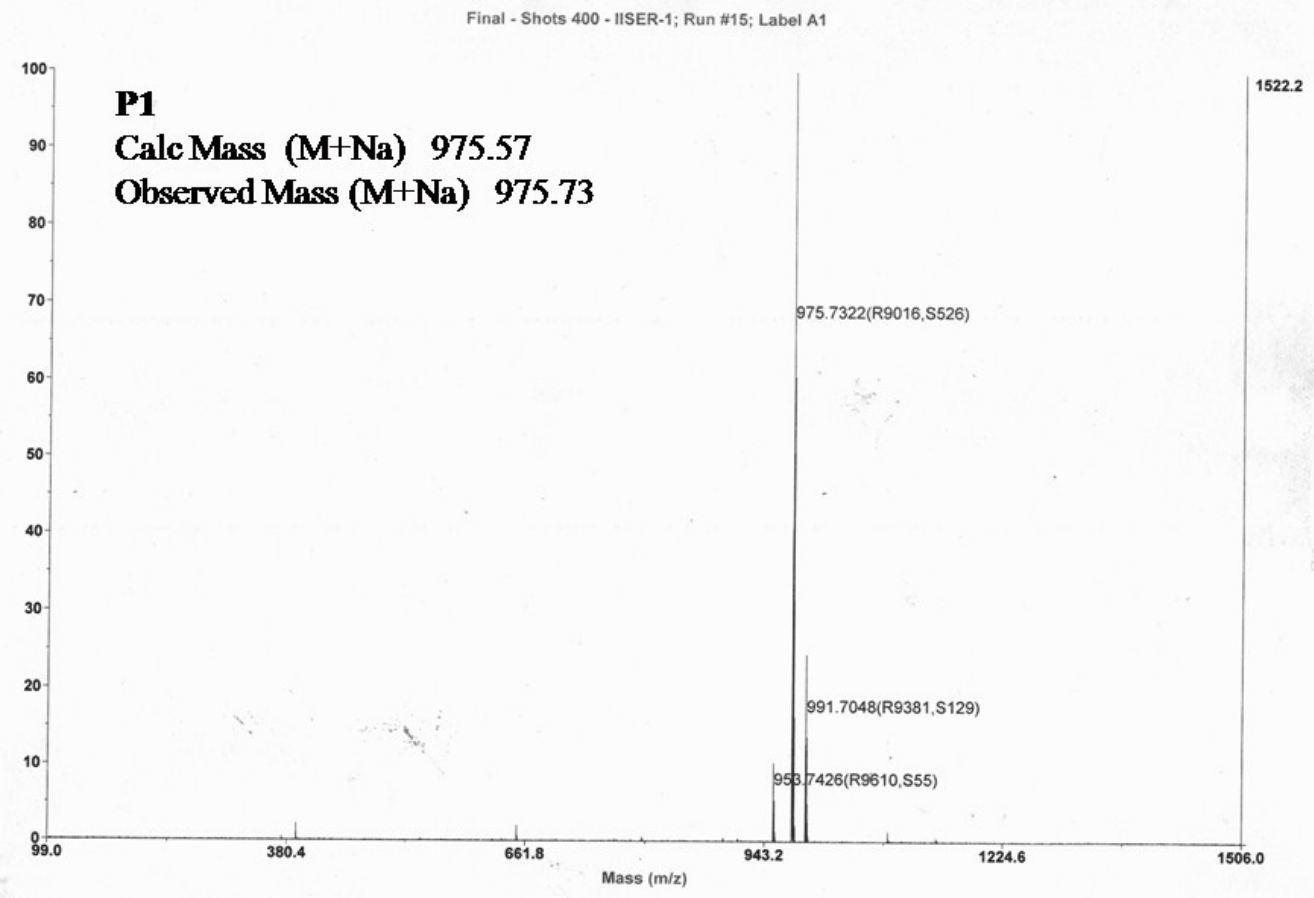

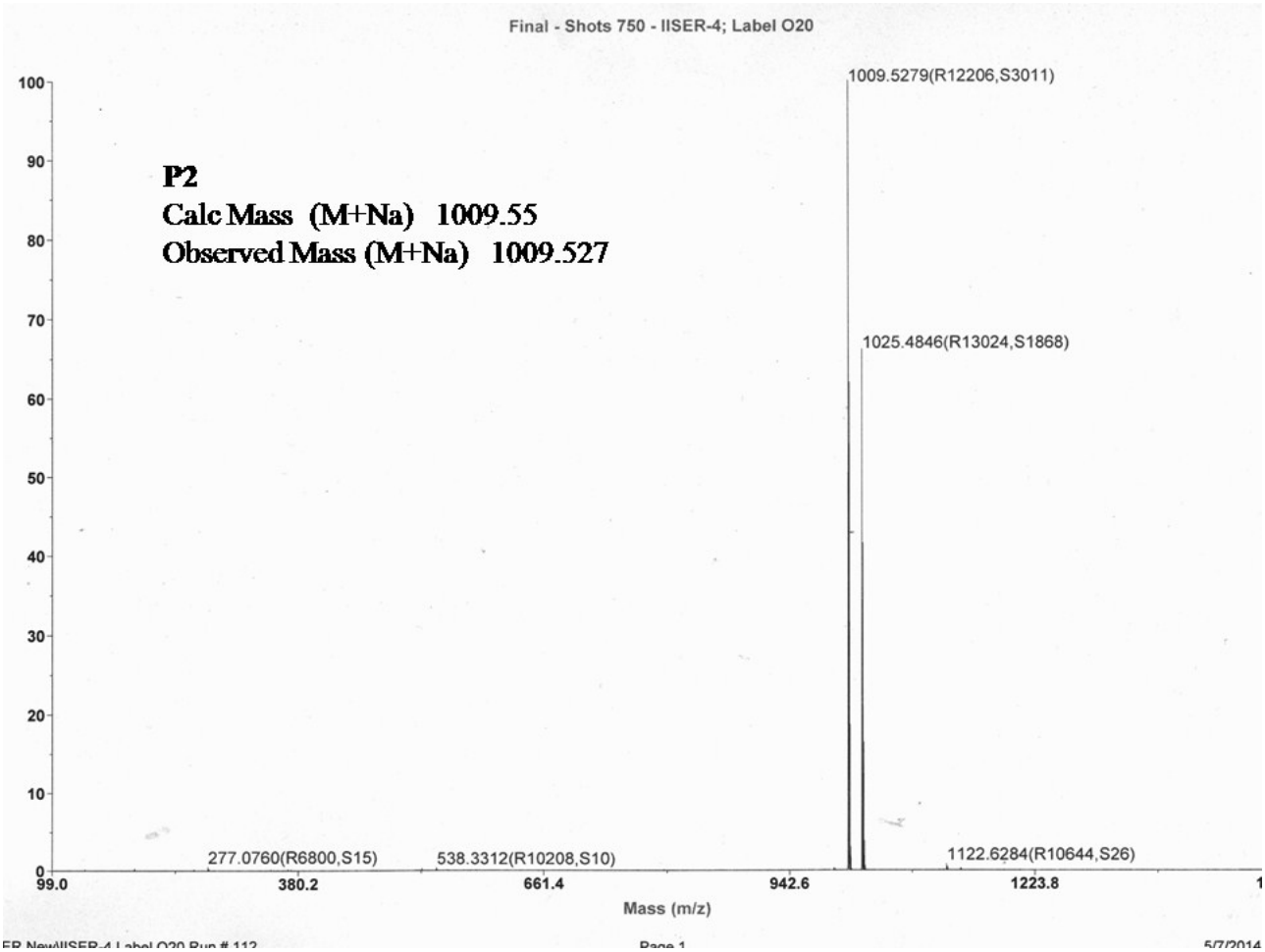
Final - Shots 750 - IISER-4; Label O20
1009.5279(R12206,S3011)
P2
Calc Mass (M+Na) 1009.55
Observed Mass (M+Na) 1009.527
1025.4846(R13024,S1868)
277.0760(R6800,S15)
538.3312(R10208,S10)
1122.6284(R10644,S26)
100
90
80
70
60
50
40
30
20
10
0
99.0
380.2
661.4
942.6
1223.8
Mass (m/z)